ISSN 1392 - 1207. MECHANIKA. 2012 Volume 18(4): 415-423

Mixed convection MHD flow of nanofluid over a non-linear stretching sheet with effects of viscous dissipation and variable magnetic field

M. Habibi Matin*, M. Dehsara, A. Abbassi*****

**Mechanical Engineering Department, Amirkabir University of Technology, 424 Hafez Avenue, P.O. Box, 15875-4413 Tehran, Iran, E-mail: m.habibi@aut.ac.ir*

***Mechanical Engineering Department, Amirkabir University of Technology, 424 Hafez Avenue, P.O. Box, 15875-4413 Tehran, Iran, E-mail: bm_dehsara@aut.ac.ir*

****Mechanical Engineering Department, Amirkabir University of Technology, 424 Hafez Avenue, P.O. Box, 15875-4413 Tehran, Iran, E-mail: abbassi@aut.ac.ir*

crossref http://dx.doi.org/10.5755/j01.mech.18.4.2334

Nomenclature

b - stretching rate, positive constant; $B(x)$ - magnetic field, tesla; B_0 - magnetic rate, positive constant; C_p - specific heat at constant pressure, J/(kg K); Ec - Eckert number, $u_w(x)^2 / C_p(T_w - T_\infty)$; f - dimensionless velocity variable; g - gravitational acceleration, m/s^2; Gr_x - Grashof number, $g(T_w - T_\infty)\beta_f / \nu_f^2$; k - thermal conductivity, W/(m K); m - index of power law velocity, positive constant; Mn - magnetic parameter, $2\sigma B_0^2 / \rho_\infty b(m+1)$; Pr - Prandtl number, $\mu_f (C_p) / k_f$; Re_x - local Reynolds number, $\rho_f u_w(x) x / \mu_f$; T - temperature variable, K; T_w - given temperature at the sheet, K; T_∞ - temperature of the fluid far away from the sheet, K; ΔT - sheet temperature, K; u - velocity in x-direction, m/s; u_w - velocity of the sheet, m/s; v - velocity in y-direction, m/s; X - horizontal distance, m; Y - vertical distance, m; ψ - stream function, m^2/s; υ - kinematic viscosity, m^2/s; β - stretching parameter, $2m/m+1$; β_f - thermal expansion coefficient of the basic fluid, K^{-1}; β_s - thermal expansion coefficient of the basic nanoparticle, K^{-1}; β_{nf} - thermal expansion coefficient of the basic nanofluid, K^{-1}; μ - dynamic viscosity , kg/(m s); ρ - density, kg/m^3; σ - electrical conductivity, mho/s; θ - dimensionless temperature variable, $T - T_\infty / T_w - T_\infty$; ϕ - solid volume fraction, (m^3)$_s$/m^3; α - thermal diffusivity, m^2/s; ρC_p - heat capacitance of the basic fluid, J/(m^{3}K);
Subscripts: f - basic fluid; s - nanoparticle; nf - nanofluid.

1. Introduction

Many recent studies have been focused on the problem of magnetic field effect on laminar mixed convection boundary layer flow over a vertical non-linear stretching sheet [1-3]. Some industrial examples of the problem are extrusion processes, cooling of nuclear reactors, glass fiber production and crystal growing. Malarvizhi et al. [4], have investigated free and mixed convection flow over a vertical plate with prescribed temperature and heat flux. Kayhani, Khaje and Sadi [5] studied the natural convection boundary layer along impermeable inclined surfaces embedded in porous medium. Mohebujjaman et al. [6], studied magneto hydrodynamics (MHD) heat transfer mixed convection flow along a vertical stretching sheet in the presence of magnetic field with heat generation. Also, Kumaran et al. [7], studied transition of MHD boundary layer flow past a stretching sheet. Fadzilah et al. [8] have investigated numerically free convection boundary layer in a Viscous Fluid. Salleh et al. [9] studied forced boundary layer Flow at a Forward Stagnation Point. The study by Prasad [10], has taken into account the effects of temperature dependent properties on the MHD forced convection over a non-linear stretching plate. In recent years, convective heat transfer from nanofluids has been noticeable. Conventional fluids, such as water, ethylene glycol mixture and some types of oil have low heat transfer coefficient, the reason for which might be related to the low conduction coefficient of these fluids. Choi [11], was the first person who utilizes nanofluid. Choi et al. [12] affirmed that the addition of a one percent by volume of nanoparticles to usual fluids increases the thermal conductivity of the fluid up to approximately two times. Recently several modeling of the natural or mixed convection of nanofluids have been investigated numerically. Ho et al. [13] studied the effect of natural convection of nanofluid in an enclosure due to uncertainties in viscosity and thermal conductivity. Ghasemi and Aminossadati [14] presented the numerical solution of natural convection in an inclined enclosure filled with a water-CuO nanofluid. Maiga et al. [15] studied the effect of nanofluid on forced convection heat transfer enhancement. Wang and Mujumdar [16-18] reported numerical investigations, experiments and applications of nanofluids, which are very useful and can be applied. Therefore, the mixed convection heat transfer of nanofluid over a vertical stretching sheet in the presence of variable magnetic field and viscous dissipation effects were not investigated. The importance of viscous dissipation term is due to the increase in friction coefficient, when solid particles are in contact with the solid plate. Also, the presence of nanoparticles in the magnetic field may have interesting results.

In the present study, mixed convection MHD flow of nanofluid along a non-linear stretching sheet with the presence of viscous dissipation and variable magnetic field is investigated. The nanofluid is assumed to be homogeneous with average physical properties of basic fluid and nanoparticles. The governing boundary layer equations are transformed into non-linear ordinary differential equations by considering suitable similarity variables. The resultant similarity equations are solved using an implicit finite-difference scheme known as Keller Box method.

2. Mathematical analysis

A steady state two dimensional mixed convection boundary layer flow of nanofluid from a vertically stretching sheet with variable magnetic field and viscous dissipation effect is considered.

The nanofluid is assumed as a homogeneous fluid with average physical properties of basic fluid and nanoparticles. Therefore the nanofluid is assumed to be a single phase solution. In other words we have just investigated the macroscopic behavior of the nanofluid in the mixed convection boundary layer. As it can be seen in [19] and [20], these assumptions are used for natural convection boundary layer flow of nanofluid over a vertical plate. The nanofluid is composed of solid particles suspended in dense fluid (e.g. aqueous suspended) i.e., we have a mixture. Therefore the gravity force applies to the whole nanofluid as a body force. A quiescent incompressible and electrically conducting fluid in the presence of a magnetic field $B(x)$ perpendicular to the sheet is taken into account along with the dissipation effect. Fig. 1. shows the schematic view of the physical model and coordinates of the system.

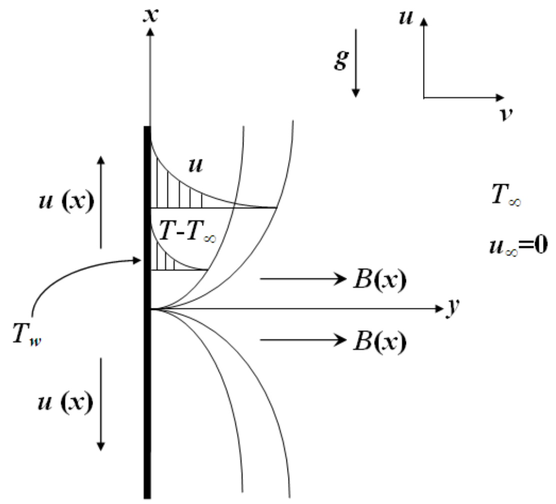

Fig. 1 Schematic of the physical model and coordinate system

The x-axis is assumed to be in the direction of the flow and the y-axis to be perpendicular to it. The temperature at the sheet (T_w) is larger than the ambient temperature (T_∞). The base fluid is water and the considered nanoparticles include CuO, Cu, Al_2O_3, TiO_2, Ag and SiO_2. For incompressible viscous fluid flow, the governing equations based on the Boussinesq approximation and considering constant physical properties of the base fluid and nanoparticles can be written as

$$\frac{\partial u}{\partial x}+\frac{\partial v}{\partial y}=0 \tag{1}$$

$$u\frac{\partial u}{\partial x}+v\frac{\partial u}{\partial y}=\frac{1}{\rho_{nf}}\left(\begin{array}{l}\mu_{nf}\dfrac{\partial^2 u}{\partial y^2}+(\rho\beta)_{nf}\,g\left(T-T_\infty\right)-\\ -\sigma B(x)^2 u\end{array}\right) \tag{2}$$

$$\left(u\frac{\partial T}{\partial x}+v\frac{\partial T}{\partial y}\right)=\alpha_{nf}\frac{\partial^2 T}{\partial y^2}+\frac{\mu_{nf}}{\left(\rho C_p\right)_{nf}}\left(\frac{\partial u}{\partial y}\right)^2 \tag{3}$$

The boundary conditions are

$$\left.\begin{array}{l}u=u_w=bx^m,\, v=0,\, T=T_w,\, at\, y=0\\ u\to 0,\, T\to T_\infty,\, at\, y\to\infty\end{array}\right\} \tag{4}$$

where ρ_{nf}, μ_{nf} and α_{nf} are effective density, effective dynamic viscosity and effective diffusivity of the nanofluid, respectively [21].

$$\rho_{nf}=(1-\phi)\rho_f+\phi\rho_s \tag{5}$$

$$\mu_{nf}=\frac{\mu_f}{(1-\phi)^{2.5}} \tag{6}$$

$$(\rho\beta)_{nf}=(1-\phi)(\rho\beta)_f+\phi(\rho\beta)_s \tag{7}$$

$$\alpha_{nf}=\frac{k_{nf}}{\left(\rho C_p\right)_{nf}} \tag{8}$$

here μ_f is the dynamic viscosity of the basic fluid; ρ_f, ρ_s, $(C_p)_f$ and $(C_p)_s$ are the density of basic fluid, the density of the nanoparticle, heat capacity of the basic fluid and heat capacity of the nanoparticle, respectively; k_{nf} is the thermal conductivity of the nanofluid and $(\rho C_p)_{nf}$ is the heat capacitance of the nanofluid, which are as follows

$$\left(\rho C_p\right)_{nf}=(1-\phi)\left(\rho C_p\right)_f+\phi\left(\rho C_p\right)_s \tag{9}$$

$$\frac{k_{nf}}{k_f}=\frac{k_s+2k_f-2\phi\left(k_f-k_s\right)}{k_s+2k_f+2\phi\left(k_f-k_s\right)} \tag{10}$$

where k_f , k_s are the thermal conductivity of the base fluid and nanoparticles, respectively.

The functional form of magnetic field is as $B(x)=B_0\sqrt{x^{m-1}}$ [22, 23].

The following dimensionless similarity variable is used to transform the governing equations into the ordinary differential equations

$$\eta=\frac{y}{x}\sqrt{\frac{m+1}{2}}\left(Re_x\right)^{\frac{1}{2}} \tag{11}$$

where $Re_x=\dfrac{\rho_f u_w(x)}{\mu_f}x$.

The dimensionless stream function and dimensionless temperature are

$$f(\eta)=\frac{\psi(x,y)\left(Re_x\right)^{\frac{1}{2}}}{u_w(x)} \tag{12}$$

$$\theta(\eta)=\frac{T-T_{\infty}}{T_w-T_{\infty}} \quad (13) \qquad u=\frac{\partial\psi}{\partial y}, v=-\frac{\partial\psi}{\partial x} \quad (14)$$

where the stream function $\psi(x,y)$ satisfies the Eq. (1).

By applying the similarity transformation parameters, the momentum Eq. (2) and energy Eq. (3) can be written as

$$f_{\eta\eta\eta}+(1-\phi)^{2.5}\left\{\left[(1-\phi)+\phi\left(\frac{\rho_s}{\rho_f}\right)\right]\left(ff_{\eta\eta}-\beta f_{\eta}^2\right)-Mnf_{\eta}+\left[(1-\phi)+\phi\left(\frac{(\rho\beta)_s}{(\rho\beta)_f}\right)\right]\left(\frac{Gr}{Re_x^2}\right)\theta\right\}=0 \quad (15)$$

$$\frac{1}{(1-\phi)+\phi\left(\frac{(\rho\beta)_s}{(\rho\beta)_f}\right)}\left[\frac{k_{nf}}{k_f}\theta_{\eta\eta}+\frac{1}{(1-\phi)^{2.5}}Ec\,Pr\,f_{\eta\eta}^2\right]+Pr\,f\,\theta_{\eta}=0 \quad (16)$$

Therefore, the transformed boundary conditions are

$$f_{\eta}(0)=1,\ f(0)=0, \theta(0)=1 \quad (17)$$

$$f_{\eta}(\infty)=0, \theta(\infty)=0 \quad (18)$$

The dimensionless parameters of Gr/Re^2, Nu and C_f are the Richardson number, Nusselt number and stretching sheet friction coefficient respectively. They are defined as

$$\left.\begin{aligned}&\frac{Gr}{Re_x{}^2}=\frac{g(T_w-T_{\infty})\beta_f}{u_w(x)^2x^2}, Nu=-\sqrt{\frac{m+1}{2}Re_x}\,\theta_{\eta}(0)\\&C_f=-\sqrt{\frac{2(m+1)}{Re_x}}f_{\eta\eta}(0)\end{aligned}\right\}. \quad (19)$$

3. Numerical method

Two dimensional equations of flow and energy for a vertical, non linear stretching sheet have been considered. These equations include, the viscous dissipation and variable (non linear) magnetic field. Then, they were transformed into similarity form. From similarity solution, two non linear coupled equations were derived. These two equations are converted into five first order equations. Then the system of first-order equations is solved numerically using an efficient implicit finite-difference scheme known as Keller Box method. The non-linear discretized system of the equations is linearized, using Newton's method [24-26]. The system of obtained equations is a block-tridiagonal which is solved using the block-tridiagonal-elimination technique. A step size of $\Delta\eta$ = 0.005 was selected to satisfy the convergence criterion of 10^{-4} in all cases. In this solution, $\eta_{\infty} = 5$ is sufficient to apply perfect effect of boundary layer.

4. Results and discussion

Here, MHD mixed convection heat transfer of nanofluid along a vertical, non-linear stretching sheet has been considered. The effect of volume fraction of nano particles, stretching, MHD effects and non dimensional Eckert and Richardson numbers are considered. Also, the effects of the type nano particles on thermal and hydrodynamic boundary layers based on similarity variables have been shown.

Table 1 depicts a comparison between the present results and Hamad's results [19]. As illustrated in Table 1 there is only a small difference between the results, which confirms the validity of the present results.

In Table 2, thermal properties of nanoparticles of the present work are seen. Also, Tables 3 and 4 show the values of Nusselt number and stretching sheet friction coefficient for different governed physical parameters and different nanoparticles.

Table 1

Comparison between the present results with results by Hamad et al. [19] for various nanoparticles in water (Pr = 6.2) at Ec = 0, Mn = 0, Gr/Re^2 = 1, β = 1

	ϕ	$f_{\eta\eta}(0)$		$-\theta_{\eta}(0)$	
		Hamad et al.	Present results	Hamad et al.	Present results
Al_2O_3	0.0	0.4427	0.4389	0.8995	0.8876
	0.2	0.3190	0.3208	0.7113	0.7164
Ag	0.0	0.4382	0.4396	0.9005	0.9017
	0.2	0.3053	0.3084	0.7132	0.7156
Cu	0.0	0.4367	0.4401	0.9492	0.9511
	0.2	0.3059	0.3072	0.8481	0.8510

Table 2

Thermo-physical properties of water and nanoparticles [19, 27-29]

Physical Properties	Fluid Phase (water)	SiO_2	Cu	Ag	Al_2O_3	TiO_2	CuO
ρ, kg m^{-3}	997.1	3970	8933	10500	3970	4250	6500
C_p, J kg^{-1}K^{-1}	4179	765	385	235	765	686.2	540
$\beta\times10^5$, K^{-1}	21.0	0.63	1.67	1.89	0.85	0.90	0.85
k, W m^{-1}K^{-1}	0.613	36.0	401	429	40	8.9538	18.0

Table 3

Skin friction coefficient and Nusselt number for different values of the physical parameters. SiO_2-Water, Pr = 6.2

ϕ	β	***Ec***	*Mn*	$Gr/Re^2 << 1$		$Gr/Re^2 = 1$		$Gr/Re^2 >> 1$	
				C_f	***Nu***	C_f	***Nu***	C_f	***Nu***
0.2	1	0.02	0.50	0.0949	6.6746	0.0696	7.4707	0.0011	8.9152
			0.75	0.1009	7.9201	0.0776	8.8526	0.0120	10.6034
			1.0	0.1065	9.1075	0.0849	10.1115	0.0234	12.0412
ϕ	β	*Mn*	***Ec***	C_f	***Nu***	C_f	***Nu***	C_f	***Nu***
0.2	1.0	1.0	0	0.1065	9.6732	0.0850	10.5207	0.0238	12.2357
			0.10	0.1064	6.8558	0.0844	8.5015	0.0217	11.2921
			0.20	0.1063	4.0472	0.0837	6.5427	0.0198	10.4268
ϕ	***Ec***	*Mn*	β	C_f	***Nu***	C_f	***Nu***	C_f	***Nu***
0.2	0.02	1.0	-1.0	0.0251	5.6558	0.0087	6.7544	0.0485	7.9912
			0.0	0.0579	6.8273	0.0398	7.6005	0.0119	9.0457
			1.0	0.1065	9.1075	0.0849	10.1115	0.0234	12.0412
β	***Ec***	*Mn*	ϕ	C_f	***Nu***	C_f	***Nu***	C_f	***Nu***
1	0.02	1.0	0.0	0.1065	9.1075	0.0849	10.1115	0.0234	12.0412
			0.1	0.0955	7.2426	0.0793	7.8262	0.0318	9.0896
			0.2	0.0831	5.8316	0.0716	6.0776	0.0366	6.6858

Table 4

Skin friction coefficient and Nusselt number for different values of the physical parameters and different kind of nanoparticles. Mn = 1.0, Pr = 6.2, $\beta = 1.0$, $\phi = 0.20$

	$Gr/Re^2 << 1$		$Gr/Re^2 = 1$		$Gr/Re^2 >> 1$	
	C_f	***Nu***	C_f	***Nu***	C_f	***Nu***
Water	0.1039	3.8975	0.0602	8.6312	-0.0614	11.6052
SiO_2	0.1007	2.6564	0.0661	6.2364	-0.0296	9.5413
Cu	0.1143	1.5406	0.0793	5.3308	-0.0159	9.2215
Ag	0.1182	1.1091	0.0828	4.9909	-0.0131	9.0091
Al_2O_3	0.1007	2.6631	0.0659	6.2476	-0.0301	9.5323
TiO_2	0.1016	2.4820	0.0670	6.2252	-0.0283	9.7045
CuO	0.1079	2.0169	0.0738	5.7444	-0.0196	9.5077

In Figures f_n is non dimensional velocity which is 1 on the sheet and also is zero in a distance sufficiently far away. Similarly, θ implied to non dimensional temperature with the same limits of the non dimensional velocity.

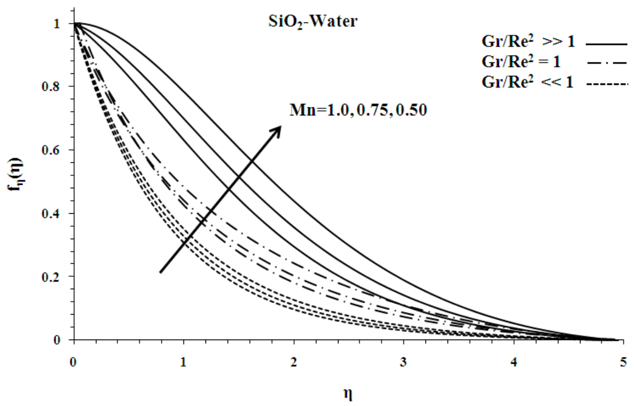

Fig. 2 Dimensionless velocity profiles for different values of Richardson number and magnetic parameter. Ec = 0.20, $\beta = 1.0$, Pr = 6.2, $\varphi = 0.20$

Fig. 2 illustrates the effect of magnetic parameter on the non dimensional velocity in presence of Richardson number. As it is seen, when Richardson number increases, the velocity boundary layer thickness also increases which shows low shear stress on the wall. The reason is due to the fact that the higher the Richardson, the more natural convection, which follows the reduction in the velocity gradient. Also, a decrease in magnetic parameter causes an increase in the boundary layer thickness. The phenomenon is due to the effect of Lorentz force which causes fluid momentum amplification and as a result, higher velocity gradient is created on the sheet. Also, it can be seen that increasing Richardson number and stable natural convection, the effect of magnetic parameter becomes more important.

In Fig. 3 the non dimensional velocity profile has been shown for different Richardson numbers with the variation of volume fraction of nanoparticles. As evident, when Richardson number is not higher than unity, within whole boundary layer thickness the increase in nanoparticle volume fraction causes reduction in velocity boundary layer thickness. While, at high Richardson numbers, the increase in nanoparticles volume fraction near the wall causes an increase in velocity profile.

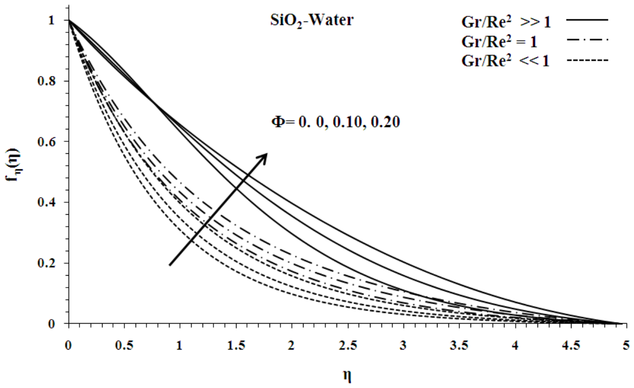

Fig. 3 Dimensionless velocity profiles for different values of Richardson number and solid volume fraction. Mn = 1.0, Ec = 0.20, $\beta = 1.0$, Pr = 6.2

As can be seen in Fig. 4, when magnetic parameter is changed between 1 and -1 the velocity boundary layer increases. In addition, it can be understood that the stretching parameter has more affects on velocity profile for Richardson numbers higher than unity or equal to unity.

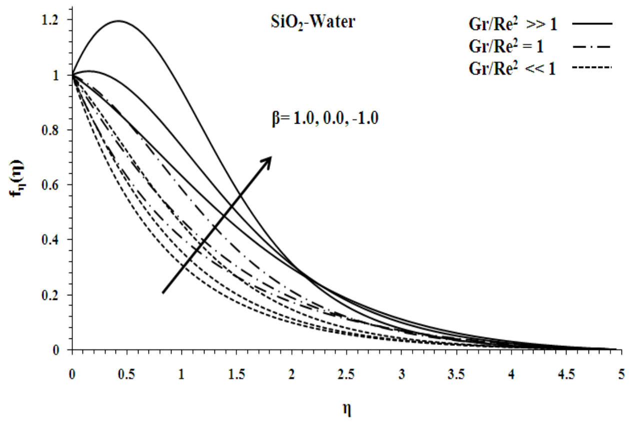

Fig. 4 Dimensionless velocity profiles for different values of Richardson number and stretching parameter. Mn = 1.0, Ec = 0.20, Pr = 6.2, $\phi = 0.20$

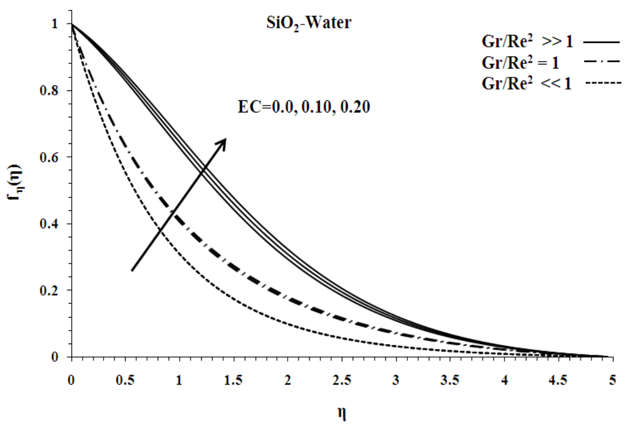

Fig. 5 Dimensionless velocity profiles for different values of Richardson and Eckert numbers. Mn = 1.0, Pr = 6.2, $\beta = 1.0$, $\phi = 0.20$

Fig. 5 shows the effect of Eckert number with Richardson number on velocity profile. As can be seen, the effect of Eckert number on boundary layer thickness is negligible at Richardson numbers lower than unity. The reason which might be associated to this is that natural convection is closer to forced convection flow and the order of magnitude of inertia forces on velocity is more than shear forces, while at Richardson numbers higher than unity, the increase in Ec number causes the boundary layer thickness becomes thicker.

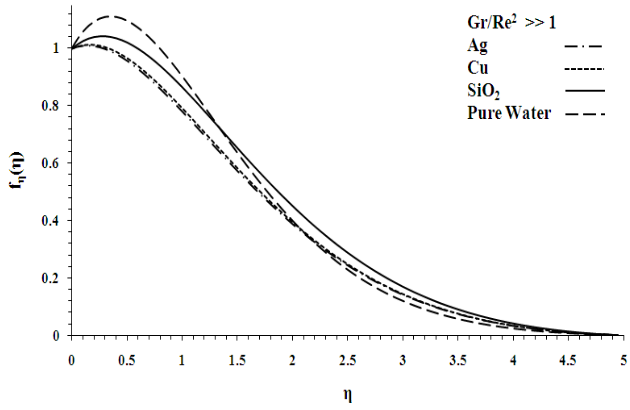

Fig. 6 Dimensionless velocity profiles for different types of nanofluids when Mn = 1.0, Ec = 0.20, Pr = 6.2, $\beta = 1.0$, $\phi = 0.20$

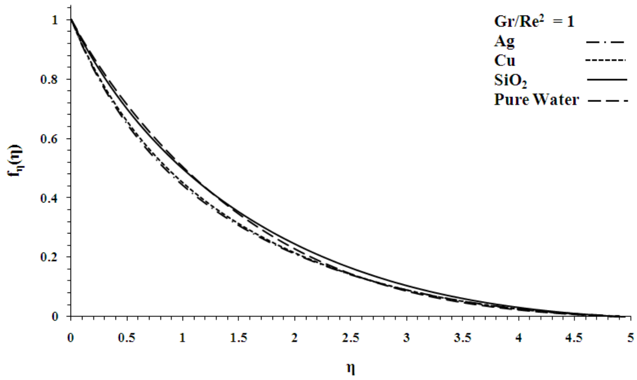

Fig. 7 Dimensionless velocity profiles for different types of nanofluids. Mn = 1.0, Ec = 0.20, Pr = 6.2, $\beta = 1.0$, $\phi = 0.20$

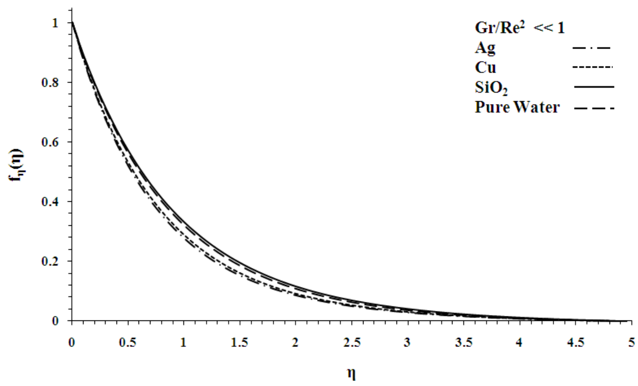

Fig. 8 Dimensionless velocity profiles for different types of nanofluids. Mn = 1.0, Ec = 0.20, Pr = 6.2, $\beta = 1.0$, $\phi = 0.20$

Figs. 6-8 show, velocity distribution profiles for various three types of used nanoparticles such as Cu, Ag, SiO_2 and pure water. In these figures, it is obvious that, boundary layer thickness changes with the change of nanoparticle type. Of course, the order of magnitude of this variation is relatively low, and main reason of this variation is different physical and mechanical properties of nanoparticles such as dynamic viscosity, density and expansion coefficients.

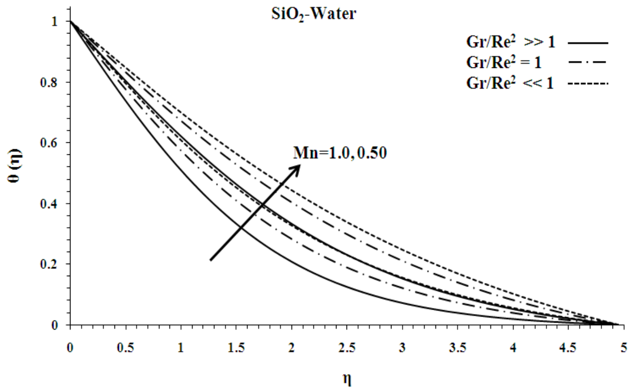

Fig. 9 Dimensionless temperature profiles for different values of Richardson number and magnetic parameter. Ec = 0.20, Pr = 6.2, $\beta = 1.0$, $\phi = 0.20$

In Fig. 9, the non dimensional temperature profiles versus variation of magnetic parameter and Richardson numbers have been plotted. As it is seen, an increase in magnetic parameter causes an increase in the thermal boundary layer. This increase is due to the Laurent forces effect. The Laurent force increases the nanofluid resistance, because of intermediate shear layer which causes increase of temperature. By considering the Richardson number, this condition is the same for natural, forced and mixed convection. Also, an increase in Richardson number causes a decrease in thermal boundary layer, which follows the increase in temperature gradient profile for different Eckert numbers. As is seen, the on the wall and as a result, heat transfer increases.

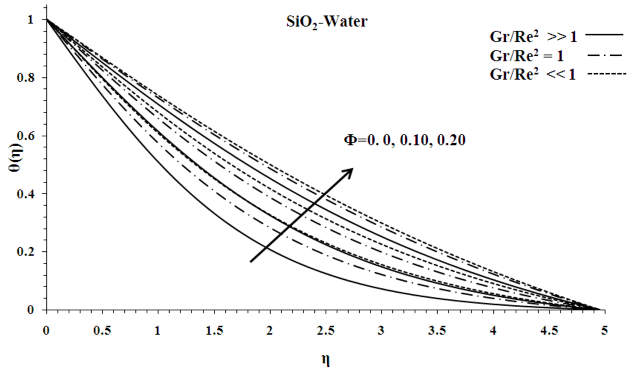

Fig. 10 Dimensionless temperature profiles for different values of Richardson number and solid volume fraction. Mn = 1.0, Ec = 0.20, Pr = 6.2, $\beta = 1.0$

Fig. 10 shows the variation of SiO_2 volume fraction on the temperature distribution for different Richardson numbers. As can be seen, the increase in volume fraction has caused the temperature profiles to shift up for all different Richardson numbers. The reason can be the increase in nanoparticles friction. Because, by increasing the volume fraction, momentum and contact between nano solid particles would increase. Also, more SiO_2 particles cause more contact between solid particles and base fluid and finally the thicker thermal boundary layer.

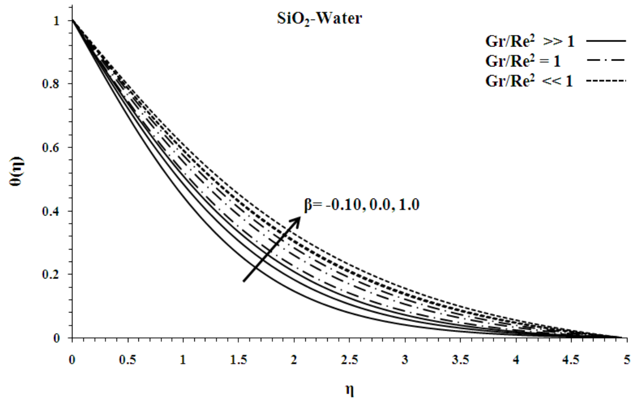

Fig. 11 Dimensionless temperature profiles for different values of Richardson number and stretching parameter. Mn = 1.0, Ec = 0.20, Pr = 6.2, $\phi = 0.20$

The non dimensional temperature profiles versus different stretching parameter (β) origin velocity and also the values of 0 and 1 show linear and constant velocity for stretching sheet respectively. By considering the Fig. 11, it is seen that the increase in stretching parameter has caused the thermal boundary layer.

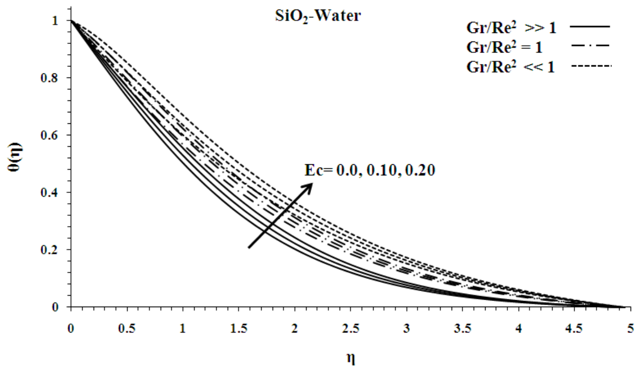

Fig. 12 Dimensionless temperature profiles for different values of Richardson and Eckert numbers. Mn = 1.0, Ec = 0.20, Pr = 6.2, $\beta = 1.0$, $\phi = 0.20$

Fig. 12 shows the variation of temperature increase in Ec number caused the increase in fluid temperature. Because, the higher the Ec number, the higher the viscous dissipation effect in thermal boundary layer.

In addition, Figs. 13-15 show temperature profiles for some types of nanoparticles with water as base fluid. It can be found that nanoparticles cause an increase in thermal boundary layer of natural, forced and mixed convection. As a result, temperature gradient on the wall decreases, which is in fact what was expect. Therefore, it can be said that the effect of existence of nano particles is to cause velocity and temperature to shift to the upper bands. This situation recovers the condition of shear forces and heat transfer of the sheet.

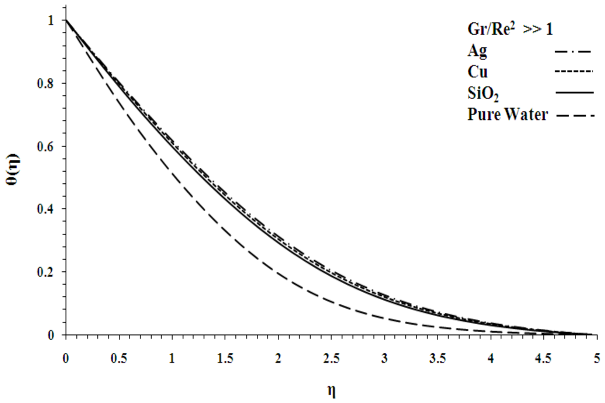

Fig. 13 Dimensionless temperature profiles for different for different types of nanofluids when *Mn* = 1.0, *Ec* = 0.20, *Pr* = 6.2, $\beta = 1.0$, $\phi = 0.20$

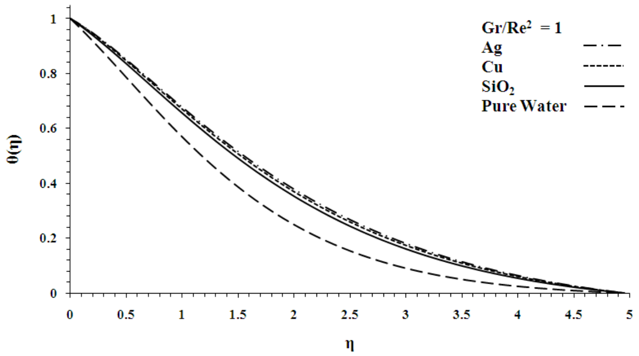

Fig. 14 Dimensionless temperature profiles for different for different types of nanofluids. *Mn* = 1.0, *Ec* = 0.20, *Pr* = 6.2, $\beta = 1.0$, $\phi = 0.20$

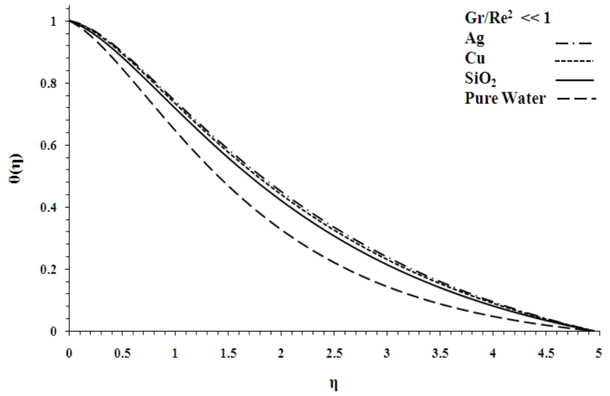

Fig. 15 Dimensionless temperature profiles for different for different types of nanofluids. *Mn* = 1.0, *Ec* = 0.20, *Pr* = 6.2, $\beta = 1.0$, $\phi = 0.20$

5. Conclusions

In this work, an analytical and numerical study of mixed convection with the effects of MHD flow of nanofluid over a non-linear stretching sheet and viscous dissipation was considered. The nanofluid was made of such nanoparticles as SiO_2, TiO_2, CuO and Ag with pure water as a base fluid. The nanofluid was assumed as a homogeneous fluid with average physical properties of basic fluid and nanoparticles. The values of Nusselt and drag coefficients for different non dimensional parameters of stretching and magnetic field effects, Eckert and Richardson numbers and volume fraction of nanoparticles were given. The results of these parameters compared to each other. The results show that, adding nanoparticles to the base fluids in forced, natural and mixed convection would cause a reduction in shear force and a decrease in stretching sheet heat transfer coefficient. Also, in nanofluid the decrease in magnetic parameter and increase in Eckert number cause better thermal conditions. In addition, using Ag nanoparticles showed better thermal conditions in comparison with other nanoparticles.

References

1. **Fisher; E.G.** 1976. Extrusion of Plastics, Wiley, New York, 344 p.
2. **Altan, T.; Oh, S.; Gegel, H.** 1979. Metal Forming Fundamentals and Applications, American Society of Metals, Metals Park, OH, 353 p.
3. **Tadmor, Z.; Klein, I.** 1970. Engineering principles of plasticating extrusion, Polymer Science and Engineering Series, Van Nostrand Reinhold, New York.
4. **Malarvizhi, G.; Ramanaiah, G.; Pop, I.** 1994. Free and mixed convection about a vertical plate with prescribed temperature or heat flux, ZAMM 74: 129-131. http://dx.doi.org/10.1002/zamm.19940740216.
5. **Kayhani, M.H.; Khaje, E., Sadi, M.** 2011. Natural convection boundary layer along impermeable inclined surfaces embedded in porous medium, scientific journal Mechanika 17(1): 64-70.
6. **Mohebujjaman, M.; Khaleque, T.S.; Samad, M.A.** MHD heat transfer mixed convection flow along a vertical stretching sheet in presence of magnetic field with heat generation, Int. J. Basic & Appl. Sci. 10(2): 133-142.
7. **Kumaran, V.; Kumar, A.V. ; Pop I.** 2010. Transition of MHD boundary layer flow past a stretching sheet, Comm. Nonlinear Sci. Numer. Simul. 15: 300-311. http://dx.doi.org/10.1016/j.cnsns.2009.03.027.
8. **Fadzilah, Md. A.; Nazar, R.; Norihan, Md. A.** 2009. Numerical investigation of free convective boundary layer in a viscous fluid, Amer. J. of Sci. Res. 5: 13-19.
9. **Salleh, M.Z.; Nazar, R.; Ahmad, S.** 2008. Numerical solutions of the forced boundary layer flow at a forward stagnation point, Eur. J. Sci. Res. 19: 644-653.
10. **Prasad, K.V.; Vajravelu, K.; Datti, P.S.** 2010. Mixed convection heat transfer over a non-linear stretching surface with variable fluid properties, Int. J. Non-Linear Mech. 45: 320-330. http://dx.doi.org/10.1016/j.ijnonlinmec.2009.12.003.
11. **Choi.; S.U.S.** 1995. Enhancing thermal conductivity of fluids with nanoparticles, in: The Proceedings of the 1995 ASME International Mechanical Engineering Congress and Exposition, San Francisco, USA, ASME, FED 231/MD 66: 99-105.
12. **Choi, S.U.S.; Zhang, Z.G.; Yu, W.; Lockwood, F.E.; Grulke, E.A.** 2001. Anomalously thermal conductivity enhancement in nanotube suspensions, Appl. Phys. Lett. 79:2252-2254. http://dx.doi.org/10.1063/1.1408272.
13. **Ho, C.J.; Chen, M.W.; Li, Z.W.** 2007. Effect of natural convection heat transfer of nanofluid in an enclosure due to uncertainties of viscosity and thermal conductivity, In. Proc. ASME/JSME Thermal Engng. Summer Heat Transfer Conf. – HT 1: 833-841.

http://dx.doi.org/10.1080/10407780902864623.

14. **Ghasemi, B.; Aminossadati, S.M.** 2009. Natural convection heat transfer in an inclined enclosure filled with a water-Cuo nanofluid, Numer. Heat Transfer; Part A: Applications 55 : 807-823.
15. **Maiga, S.E.B.; Palm, S.J.; Nguyen, C.T.; Roy, G.; Galanis, N.** 2005. Heat transfer enhancement by using nanofluids in forced convection flow, Int. J. Heat Fluid Flow 26: 530-546. http://dx.doi.org/10.1016/j.ijheatfluidflow.2005.02.004.
16. **Wang, X.-Q.; Mujumdar, A.S.** 2007. Heat transfer characteristics of nanofluids: a review, Int. J. Thermal Sci. 46: 1-19. http://dx.doi.org/10.1016/j.ijthermalsci.2006.06.010.
17. **Wang, X.-Q.; Mujumdar, A.S.** 2008. A review on nanofluids – Part I: theoretical and numerical investigations, Brazilian J. Chem. Engng. 25: 613-630. http://dx.doi.org/10.1590/S0104-66322008000400001.
18. **Wang, X.-Q.; Mujumdar, A.S.** 2008. A review on nanofluids – Part II: experiments and applications, Brazilian J. Chem. Engng. 25: 631-648. http://dx.doi.org/10.1590/S0104-66322008000400002.
19. **Hamad, M.A.A.; Pop, I.; Ismail, A.I.Md.** 2011. Magnetic field effects on free convection flow of a nanofluid past a vertical semi-infinite flat plate, Nonlinear Anal.: Real World Applications 12: 1338-1346. http://dx.doi.org/10.1016/j.nonrwa.2010.09.014.
20. **Ahmad, S.; Pop, I.** 2010. Mixed convection boundary layer flow from a vertical flat plate embedded in a porous medium filled with nanofluids, Int. Comm. Heat Mass Transfer 37: 987-991. http://dx.doi.org/10.1016/j.icheatmasstransfer.2010.06.004.
21. **Aminossadati, S.M.; Ghasemi, B.** 2009. Natural convection cooling of a localised heat source at the bottom of a nanofluid-filled enclosure. Eur. J. Mech. B/Fluids 28: 630-640. http://dx.doi.org/10.1016/j.euromechflu.2009.05.006.
22. **Chiam, T.C.** 1995. Hydromagnetic flow over a surface with a power law velocity, Int. J. Eng. Sci. 33: 429-435. http://dx.doi.org/10.1016/0020-7225(94)00066-S.
23. **Devi, S.P.A.; Thiyagarajan, M.** 2006. Steady nonlinear hydromagnetic flow and heat transfer over a stretching surface with variable temperature, Heat Mass Transfer 42: 671-677. http://dx.doi.org/10.1007/s00231-005-0640-y.
24. **Cebeci, T.; Bradshaw, P.** 1977. Momentum Transfer in Boundary Layers, New York, Hemisphere Publishing Corporation, 407 p.
25. **Cebeci, T.; Bradshaw, P.** 1988. Physical and Computational Aspects of Convective Heat Transfer. New York, Springer-Verlag, 487 p. http://dx.doi.org/10.1007/978-1-4612-3918-5.
26. **Salleh, M.Z., Nazar, R.; Ahmad, S.** 2008. Numerical solutions of the forced boundary layer flow at a forward stagnation point, Eur. J. Sci. Res. 19: 644-653.
27. **Ibrahim, F.S.; Hamad, M.A.A.** 2006. Group method analysis of mixed convection boundary layer flow of a micropolar fluid near a stagnation point on a horizontal cylinder, Acta Mech. 181: 65-81. http://dx.doi.org/10.1007/s00707-005-0272-9.
28. **Abu-Nada, E.** 2009. Effect of variable viscosity and thermal conductivity of Al_2O_3–water nanofluid on heat transfer enhancement in natural convection, Int. J. Heat Fluid Flow 30: 679-690. http://dx.doi.org/10.1016/j.ijheatfluidflow.2009.02.003.
29. **Jang, S.P.; Choi**, **S.U.S.** 2007. Effects of various parameters on nanofluid thermal conductivity, ASME J. Heat Transfer 129: 617-623. http://dx.doi.org/10.1115/1.2712475.

M. Habibi Matin, M. Dehsara, A. Abbassi

MIŠRIOS KONVEKCIJOS NANOSKYSČIO MHD TEKĖJIMAS PRO NETIESINĮ PAILGINTĄ KOLEKTORIŲ ESANT KLAMPIAJAI SKLAIDA IR KINTAMAM MAGNETINIAM LAUKUI

R e z i u m ė

Straipsnyje pateikiamas analitinis ir skaitinis mišrios konvekcijos tyrimas įvertinant nanoskysčio MHD tekėjimo, per nelinijinį pailgintą kolektorių efektą ir klampiąją sklaidą. Nanoskystis yra sudarytas iš SiO_2, TiO_2, CuO ir Ag nanodalelių ir bazinio skysčio – vandens. Analizuojant problemą, ribinių sluoksnių lygtys transformacija pirmiausiai yra pakeičiama įprastomis netiesinėmis lygtimis.

Gautos lygtys yra skaitmeniškai išspręstos taikant Keller Box ir įprastą baigtinių skirtumų metodus. Detaliai ištyrinėti bedimensinių skirtingų pagrindinių parametrų, tokių kaip magnetiniai parametrai, nanodalelių tūrio frakcijos, Nusselt, Richardsono or Echerto skaičių efektai. Rezultatai parodė, kad, pridėjus nanodalelių į bazinius skysčius, priverstinė, natūrali ir mišri korekcija sumažina šlyties jėgas ir šilumos perdavimo koeficientą pailgintame kolektoriuje. Taigi, mažėjantis magnetinis parametras ir didėjantis Eckerto skaičius leidžia pagerinti šilumines sąlygas. Be to, naudojant Ag nanodaleles gaunamos geresnės šiluminės sąlygos nei naudojant kitas nanodaleles.

M. Habibi Matin, M. Dehsara, A. Abbassi

MIXED CONVECTION MHD FLOW OF NANOFLUID OVER A NON-LINEAR STRETCHING SHEET WITH EFFECTS OF VISCOUS DISSIPATION AND VARIABLE MAGNETIC FIELD

S u m m a r y

The present paper deals with an analytical and numerical study of mixed convection taking into account the effects of MHD flow of nanofluid over a non-linear stretching sheet and viscous dissipation. The nanofluid is made of such nanoparticles as SiO_2, TiO_2, CuO and Ag with pure water as a base fluid. To analyze the problem, at first the boundary layer equations are transformed into non-linear ordinary equations using a similarity transformation. The resultant equations are then solved numerically using the Keller Box method based on the implicit finite-difference method. The effects of different non-dimensional governing parameters such as magnetic parameter, nanoparticles volume fraction, Nusselt, Richardson and Eckert numbers are investigated in details. The results indicate that, by adding the nanoparticles to the base fluids in forced, natural and mixed convection would cause the reduction in shear forces and a decrease in stretching sheet heat transfer coefficient. Also, in nanofluid decreasing of magnetic parameter and increasing Eckert number would result in better thermal conditions. In addition, using the Ag nanoparticles indicate better thermal conditions in comparison with other nanoparticles.

Keywords: mixed convection, MHD, nanofluid, non-linear stretching sheet.

Received March31, 2011
Accepted June 28, 2012